Available online at www.sciencedirect.com
ScienceDirect
Scripta Materialia 63 (2010) 162–165
Scripta MATERIALIA
www.elsevier.com/locate/scriptamat

Excellent combination of strength and ductility in an Fe–9Al–28Mn–1.8C alloy

K.M. Chang, C.G. Chao and T.F. Liu*

Department of Materials Science and Engineering, National Chiao Tung University, 1001 Ta Hsueh Road, Hsinchu 30049, Taiwan, ROC

Received 3 February 2010; revised 15 March 2010; accepted 15 March 2010
Available online 20 March 2010

An optimal aging at 450 °C resulting in the subject alloy possessing a high yield strength of 1383 MPa with 32.5% elongation. With almost equivalent elongation, the yield strength was about 28% higher than that of FeAlMnC ($C \leqq 1.3$ wt.%) alloys after solution heat-treatment or controlled-rolling followed by optimal aging. Additionally, due to pre-existing fine $(Fe,Mn)_3AlC$ carbides in as-quenched alloy, the aging time required for attaining the optimal combination of strength and ductility was much less than that for FeAlMnC ($C \leqq 1.3$ wt.%) alloys.

Keywords: Spinodal decomposition; Carbides; Microstructure; Mechanical properties; FeAlMnC alloy

In previous studies, it was found that the as-quenched microstructure of the Fe–(7–10) wt.% Al–(28–32) wt.% Mn–(0.54–1.3) wt.% C alloys was single-phase austenite (γ) [1–9]. Depending on the chemical composition, the ultimate tensile strength (UTS), yield strength (YS) and elongation of the as-quenched alloys were 840–993 MPa, 410–551 MPa and 72–50%, respectively [5–8]. When the as-quenched alloy was aged at 550 °C for about 16 h, a high density of fine $(Fe,Mn)_3AlC$ carbides (κ' carbides) started to precipitate within the γ matrix and no precipitates were formed on the grain boundaries [8,9]. The resultant microstructure possessed an optimal combination of mechanical strength and ductility. With an elongation better than about 30%, values of 871–1259 MPa for UTS and 665–1094 MPa for YS could be attained [8,9]. Recently, in order to further improve the strength, small amounts of V, Nb, Mo and W have been added to the austenitic FeAlMnC ($C \leqq 1.3$ wt.%) alloys [10–13]. After solution heat-treatment or controlled-rolling followed by an optimum aging at 550 °C, the UTS and YS of the FeAlMnMC (M = V, Nb, Mo, W) alloys were significantly increased up to 1130–1220 and 890–1080 MPa, respectively, with 41–26% elongation [10–13].

Additionally, the microstructural developments of the austenitic FeAlMnC alloys with higher carbon content have also been studied by several workers [14–16]. Interestingly, a high density of fine κ' carbides could be observed in the as-quenched Fe–(7.7–9 wt.%) Al–(29–30 wt.%) Mn–(1.5–2.5 wt.%) C alloys [15,16]. The fine κ' carbides were formed within the austenite matrix by spinodal decomposition during quenching [16]. This is different from that observed in the austenitic FeAlMn(M)C ($C \leqq 1.3$ wt.%) alloys, in which the fine κ' carbides could only be observed in the aged alloys [1–9]. When the as-quenched alloy was aged at 550–800 °C, the fine κ' carbides grew within the γ matrix and a $\gamma + \kappa' \rightarrow \gamma_o$ (carbon-deficient austenite) $+ \kappa$ reaction occurred heterogeneously on the γ/γ grain boundaries. The κ phase is also an $(Fe,Mn)_3AlC$ carbide, which was formed on the grain boundaries as a coarse particle. In contrast to the studies of the microstructures, the result concerning the mechanical properties of the austenitic FeAlMnC alloys with higher carbon content is very deficient. We are aware of only one article [15], in which the tensile properties of the Fe–15 at.% Al–26 at.% Mn–8 at.% C (Fe–8.5 wt.% Al–30 wt.% Mn–2.0 wt.% C) alloy was examined. However, these examinations were only focused on the alloy in the as-annealed condition or solution heat-treated and then aged at a high temperature of 800 °C. Therefore, the main purpose of this study is an attempt to examine the tensile properties of the Fe–9 wt.% Al–28 wt.% Mn–1.8 wt.% C alloy aged at 450 °C.

The alloy was prepared in a vacuum induction furnace using pure Fe, Al, Mn and carbon powder. The

* Corresponding author. Tel.: +886 3 5131288; fax: +886 3 5713987; e-mail: tfliu@cc.nctu.edu.tw

1359-6462/$ - see front matter © 2010 Acta Materialia Inc. Published by Elsevier Ltd. All rights reserved.
doi:10.1016/j.scriptamat.2010.03.038

melt was cast into a 20 × 30 × 100 mm steel mold. After being homogenized at 1250 °C for 24 h, the ingot was hot-rolled to a final thickness of 6 mm. The plate was subsequently solution heat-treated (SHT) at 1200 °C for 2 h and then rapidly quenched into room-temperature water. The composition of the plate determined by chemical analyses was Fe–9.07 wt.% Al–28.15 wt.% Mn–1.82 wt.% C. Aging processes were carefully performed at 450 °C for various times in a vacuum heat-treated furnace followed by rapid quenching. Transmission electron microscopy (TEM) and scanning electron microscopy (SEM) were used to investigate the microstructures and the tensile fracture surface as well as free surface. TEM specimens were prepared by using a double-jet electropolisher with an electrolyte of 60% acetic acid and 40% ethanol. The average particle size and volume fraction of the fine κ′ carbides were determined by a LECO 2000 image analyzer. Tensile tests were carried out at room temperature with an Instron tensile testing machine at a strain rate of $6.7 \times 10^{-4}\ s^{-1}$. Tensile test specimens were plates having 50 mm gauge length, 12 mm width and 5 mm thickness. The YS was measured at 0.2% offset strain.

In the as-quenched condition, the microstructure of the alloy was γ phase containing fine κ′ carbides. The average particle size and volume fraction of the fine κ′ carbides were about 22 nm and 36%, respectively. The fine κ′ carbides having an $L'1_2$ structure were formed within the γ matrix by spinodal decomposition during quenching. A typical microstructure is illustrated in Figure 1. This is similar to that observed by the present workers in the as-quenched Fe–9 wt.% Al–30 wt.% Mn–2.0 wt.% C alloy [16]. When the as-quenched alloy was aged at 450 °C for 9 h, the average particle size and volume fraction of the fine κ′ carbides increased to be about 26 nm and 42%, respectively, and no grain boundary precipitates could be detected. An example is shown in Figure 2a. Figure 2b is an SEM micrograph of the alloy aged at 450 °C for 12 h, revealing that some small particles started to appear on the grain boundaries. Electron diffraction showed that the small particles were κ carbides. With increasing aging time at 450 °C, the κ carbides grew into adjacent austenite grain through a $\gamma + \kappa' \rightarrow \gamma_o + \kappa$ reaction, as shown in Figure 2c. In Figure 2c, it is clearly seen that the mixture of $(\gamma_o + \kappa)$ phases exhibited a lamellar structure.

Table 1 shows the tensile properties of the alloy in the as-quenched condition and aged at 450 °C for various times. In Table 1, it is seen that the UTS, YS and elongation of the as-quenched alloy were 1080 MPa, 868 MPa and 55.5%, respectively. When the alloy was aged at 450 °C for less than 9 h, the strength was pronouncedly increased and the elongation was slightly decreased with increasing the aging time. This is attributed to the increase of the volume fraction of the fine κ′ carbides within the γ matrix and no precipitates on the grain boundaries. When the alloy was aged at 450 °C for 12 h, the alloy could possess the high maximum UTS (1552 MPa) and YS (1423 MPa) with a good elongation of 25.8%. However, after prolonged aging at 450 °C, both the strength and ductility were drastically decreased. In order to characterize the relationship between the microstructures and tensile properties, the specimens after tensile test were examined by using SEM. Figure 3a, a fractograph of the specimen aged at 450 °C for 9 h, indicates ductile fracture with fine and deep dimples. Figure 3b is an SEM micrograph taken from the free surface in the vicinity of the fracture surface, showing that slip bands were generated over the specimen and some isolated tiny voids (indicated by arrows) were formed randomly within the grains. It is clear that these tiny voids strongly exhibited the self-stabilization under deformation. These observations are expected, because the specimen had a good elongation of 32.5%. In the specimen aged at 450 °C for 12 h, the fractograph revealed that the dimples became coarser as well as shallower, and some dimples contain one or more coarse κ carbides (indicated by arrows), as illustrated in Figure 3c. Figure 3d, an SEM micrograph of the free surface, shows that small voids (indicated by arrows) appeared primarily along the grain boundaries. However, these small voids did not link

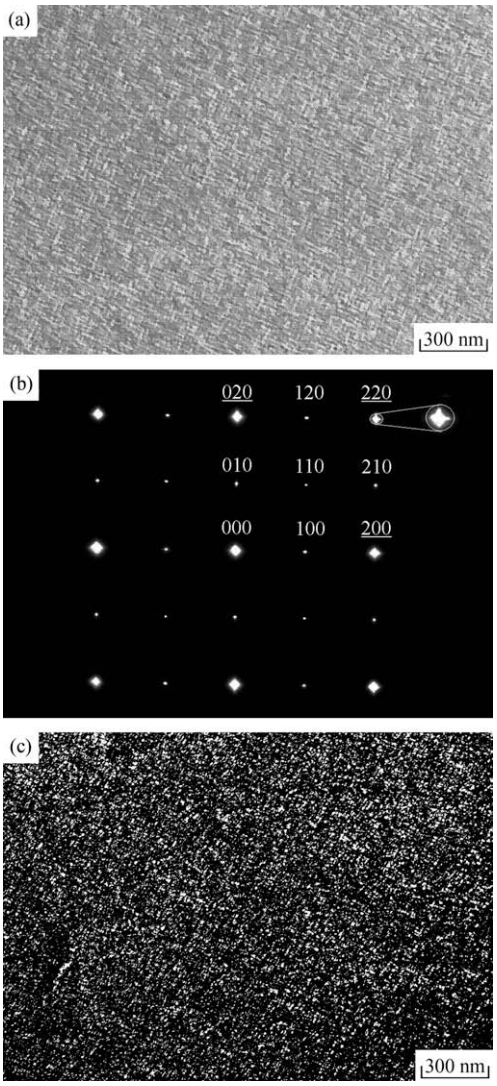

Figure 1. Transmission electron micrographs of the as-quenched alloy: (a) bright-field image; (b) a selected-area diffraction pattern taken from the mixed region of austenite matrix and fine κ′ carbides; the foil normal is [0 0 1] (hkl: γ matrix; hkl: κ′ carbide); and (c) $(1\ 0\ 0)_{\kappa'}$ dark-field image.

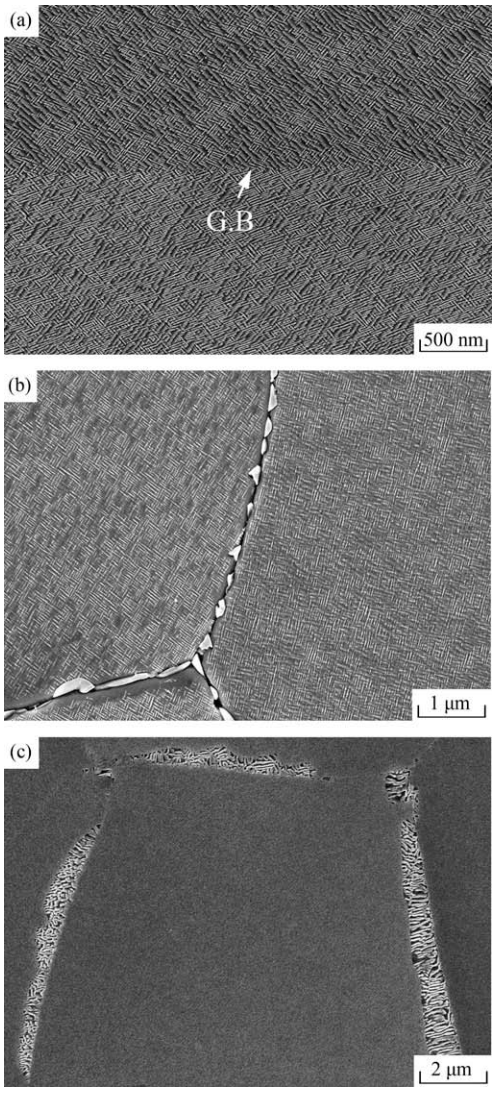

Figure 2. Scanning electron micrographs of the alloy aged at 450 °C for (a) 9 h, (b) 12 h and (c) 15 h, respectively.

up together. Therefore, under the highest strength condition, the specimen was still fairly ductile having a 25.8% elongation. However, the fracture surface and free surface of the specimen aged at 450 °C for 15 h indicated that cracks occurred mainly along the grain boundaries due to the existence of the ($\gamma_o + \kappa$) lamellar structure, as shown in Figure 3e and f. Apparently, the formation of the ($\gamma_o + \kappa$) lamellar structure on the grain boundaries deteriorated the ductility drastically.

Table 1. Tensile properties of the alloy in the as-quenched condition and aged at 450 °C for various times.

Condition	UTS (MPa)	YS (MPa)	El (%)
SHT	1080	868	55.5
450 °C, 3 h	1139	923	48.6
450 °C, 6 h	1262	1119	40.3
450 °C, 9 h	1487	1383	32.5
450 °C, 12 h	1552	1423	25.8
450 °C, 15 h	1450	1206	16.8
450 °C, 18 h	1310	1102	13.2

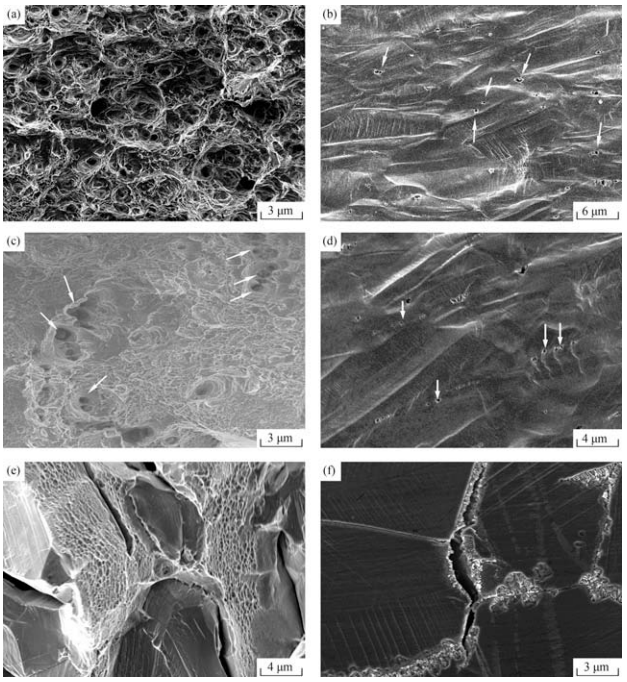

Figure 3. Scanning electron micrographs taken from the tensile fracture surface and free surface, respectively, of the specimen aged at 450 °C for (a, b) 9 h, (c, d) 12 h, and (e, f) 15 h.

Based on the preceding results, three important experimental results are discussed below.

1. Owing to contain a high density of fine κ′ carbides within the austenite matrix, the yield strength (868 MPa) of the present alloy in the as-quenched condition is much higher than that (410–551 MPa) of the as-quenched FeAlMn(M)C ($C \leqq 1.3$ wt.%) alloys [5–8]. Moreover, when the alloy was aged at 450 °C for 9 h, the YS could reach up to 1383 MPa with 32.5% elongation; aged for 12 h, the YS was 1423 MPa and elongation was 25.8%. Compared to the previous studies, it is found that with almost equivalent ductility, the present alloy can possess yield strength about 28% higher than that of the FeAlMn(M)C ($C \leqq 1.3$ wt.%) alloys after solution heat-treatment or controlled-rolling followed by the optimal aging at 450–550 °C [8–13]. The result is probably that due to higher carbon content in the present alloy, a greater amount of fine κ′ carbides could be formed within the austenite matrix during aging.
2. It is well known that the austenitic FeAlMn(M)C alloys could possess a remarkable combination of strength and ductility due primarily to the formation of fine κ′ carbides within the austenite matrix [8–13]. The as-quenched microstructure of the FeAlMn(M)C ($C \leqq 1.3$ wt.%) alloys was γ phase or γ phase with small amount of (V, Nb)C carbides, and κ′ carbides could only be formed during aging [1–13]. Therefore, the aging time required for attaining the optimal combination of strength and ductility was about 16 h at 550 °C [8–13], and more than 500 h at 450 °C [10,12]. Whereas, the time of the present alloy aged at 450 °C was only about 12 h, which was attrib-

uted to the pre-existing fine κ′ carbides within the γ matrix in the as-quenched alloy.

3. In 2004, Kimura et al. reported that when the Fe–15 at.% Al–26 at.% Mn–8 at.% C alloy was heat-treated at 1100 °C and then furnace cooled to room temperature, the alloy showed almost zero ductility due to a lot of coarse κ carbides or/and thick κ carbide film on the grain boundaries [15]. To improve the ductility, they proposed a specific heat treatment: solution treatment at 1100 °C for 1 h followed by water quenching, and subsequent aging at 800 °C for 120 h. Through the specific heat-treatment, the microstructure was a mixture of $(\gamma_o + \kappa)$ lamellar structure. Consequently, the elongation could be improved to be about 12% with YS around 675 MPa [15]. Evidently, the values of both strength and ductility are much lower than those obtained in the present alloy, and even lower than those obtained in the austenitic FeAlMn(M)C (C ≦ 1.3 wt.%) alloys [8–13]. It is therefore suggested that the $\gamma + \kappa'$ structure is more favorable for both strength and ductility than the $\gamma_o + \kappa$ lamellar structure.

Optimal aging at 450 °C resulted in the Fe–9 wt.% Al–28 wt.% Mn–1.8 wt.% C alloy possessing a high YS up to 1383 MPa with a good 32.5% elongation. Under a similar ductility level, the YS was about 28% higher than that of the FeAlMn(M)C (C ≦ 1.3 wt.%) alloys after solution heat-treatment or controlled-rolling followed by optimal aging. In addition, due to the pre-existing fine κ' carbides in the as-quenched alloy, the aging time required to attain the optimal combination of strength and ductility was much less than that of the FeAlMn(M)C (C ≦ 1.3 wt.%) alloys. When the present alloy was aged at 450 °C for a time period longer than 12 h, both the strength and ductility were drastically decreased due to the formation of the $(\gamma_o + \kappa)$ lamellar structure on the grain boundaries.

This project was supported by the National Science Council, Taiwan (NSC97-2221-E-009-027-MY3).

[1] S.M. Zhu, S.C. Tjong, Metall. Mater. Trans. A 29 (1998) 299.
[2] C.N. Hwang, C.Y. Chao, T.F. Liu, Scripta Matall. 28 (1993) 263.
[3] C.Y. Chao, C.N. Hwang, T.F. Liu, Scripta Metall. 28 (1993) 109.
[4] S.C. Tjong, S.M. Zhu, Mater. Trans. 38 (1997) 112.
[5] S.C. Chang, M.T. Jahn, J. Mater. Sci. 24 (1989) 1117.
[6] H.J. Lai, C.M. Wan, J. Mater. Sci. 24 (1989) 2449.
[7] E.K. James, Metall. Trans. A 19 (1988) 1873.
[8] W.K. Choo, J.H. Kim, J.C. Yoon, Acta Mater. 45 (1997) 4877.
[9] I. Kalashnikov, O. Acselrad, A. Shalkevich, L.C. Pereira, J. Mater. Eng. Perform. 9 (2000) 597.
[10] G.S. Krivonogov, M.F. Alekseyenko, G.G. Solov'yeva, Fiz. Metall. Metalloved. 39 (1975) 775.
[11] I.S. Kalashnikov, B.S. Ermakov, O. Aksel'rad, L.K. Pereira, Metall. Sci. Heat. Treat. 43 (2001) 493.
[12] I.S. Kalashnikov, O. Acselrad, A. Shalkevich, L.D. Chumakova, L.C. Pereira, J. Mater. Process. Tech. 136 (2003) 72.
[13] K.H. Han, Mater. Sci. Eng. A 279 (2000) 1.
[14] Y. Kimura, K. Hayashi, K. Handa, Y. Mishima, Mater. Sci. Eng. A 329 (2002) 680.
[15] Y. Kimura, K. Handa, K. Hayashi, Y. Mishima, Intermetallics 12 (2004) 607.
[16] C.S. Wang, C.N. Hwang, C.G. Chao, T.F. Liu, Scripta Mater. 57 (2007) 809.